Electrohydrodynamic Pattern Formation in Nematic Liquid Crystals by External Pure Noise

Jong-Hoon Huh

Department of Mechanical Information Science and Technology, Faculty of Computer Science and Systems Engineering, Kyushu Institute of Technology, Fukuoka 820-8502, Japan

Pure noise-induced electrohydrodynamic convections (EHCs) in nematic liquid crystals are presented in comparison with ac field-induced ones. There exists a characteristic cutoff frequency f_c^* of noise dividing EHC patterns qualitatively. Sufficiently colored noise with $f_c < f_c^*$ can induce a variety of well-ordered patterns such as Williams domains, fluctuating Williams domains, grid patterns, and dynamic scattering modes (highly developed turbulence). The amplitude of the primary pattern (Williams domains) and its wavelength are investigated with varying intensity V_N and/or cutoff frequency f_c of noise. The present noise-induced EHCs are discussed on the basis of the conventional (ac-based) Carr-Helfrich mechanism.

KEYWORGS: electrohydrodynamic convection, liquid crystal, colored noise, cutoff frequency, phase diagram

Electrohydrodynamic convections (EHCs) in nematic liquid crystals (NLCs) are one of many fascinating research topics for understanding pattern formations in spatially extended nonequilibrium dissipative systems [1,2]. In principle, they are realized by application of an electric ac field $E(t)$ across a thin slab of a NLC, as first found by Williams [3]. The frequency-dependent threshold voltage $V_c(f)$ is well explained by the Carr-Helfrich mechanism (CHM) [4]. In this mechanism, electric and visco-elastic anisotropy of NLCs plays a crucial role in inducing EHCs, unlike thermal convections in normal (isotropic) fluids [4,5]. Smoothly increasing voltage V, moreover, Williams domains (WDs), fluctuating Williams domains (FWDs), grid patterns (GPs), and dynamic scattering modes (DSMs) appear one after another [6]. Intuitively, such well-ordered patterns (e.g., WDs, FWDs, and GPs; see Fig. 4) always seem to demand a certain regular driving force (such as a sinusoidal ac field).

Now we have a question whether such a deterministic (regular) field is essential to the onset of EHC (WD) and the pattern evolution scenario. Noise can induce order in spatially extended systems? This counterintuitive question has been raised in various fields for last decades: e.g., noise-induced ordering, and nose-induced pattern and dynamics [7-9]. In particular, nose-induced pattern transition in hydrodynamic systems has been intensively studied in both theory and experiment [7-9]. In this Letter, we address *pure noise*-induced EHCs in comparison with conventional ac field-induced ones. The present phenomena should be differentiated from the noise-induced threshold shift in an additional stochastic field superposed with main deterministic ones [10-14]. In the case of the superposed fields, noise plays a role in additional stabilization and/or destabilization effects on EHCs depending on external and internal timescales of the system [10,12-14].

The well-established shadowgraph method for observation of EHCs [5,6,15] was used. A stochastic electric field $N(t)$ was applied across a thin slab of an NLC [*p*-methoxybenzylidene-*p*'-*n*-butylaniline (MBBA)] sandwiched between two parallel transparent electrodes (indium tin oxide). The Gaussian-type noise $N(t)$ was created by a wave-generating synthesizer (Hioki 7075) and amplified by a wide-range amplifier ($0 < f < 500$ kHz, FLC Electronics A600). The cutoff frequency (f_c)-dependent *colored noise* was generated from the low-pass filters of the synthesizer, which allows low-frequency signals to pass through but attenuates signals with frequencies higher than f_c. In this study, the stochastic intensity $V_N = \sqrt{< N^2(t) >} \cdot d$ and f_c of the noise $N(t)$ were used as control parameters. The thickness of a nematic slab with planar alignment [i.e., the initial director $\mathbf{n}_0 = (1,0,0)$] between transparent electrode surfaces was d = 50 μm, and the lateral (active) size was $S = 1\times1$ cm^2. All the measurements were carried out at a stable temperature (25 ± 0.2 ^{o}C) using an electrothermal control system (TH-99, Japan Hightech). At this temperature, electric conductivities and dielectric constants of MBBA were $\sigma_{//} = 6.82 \times 10^{-7}\,\Omega^{-1}\mathrm{m}^{-1}$, $\sigma_\perp = 4.30 \times 10^{-7}\,\Omega^{-1}\mathrm{m}^{-1}$, $\varepsilon_{//} = 5.26$, and $\varepsilon_\perp = 5.63$, respectively. Here, the subscripts // and $\perp$ represent the orientations parallel and perpendicular to the director of NLCs, respectively. The detail of experiment was described in our recent papers [14].

In order to obtain EHCs in a pure stochastic field, one should control material parameters (e.g., the electric conductivity) determining a critical frequency f_{cd} (dividing conductive and dielectric regimes for EHCs [5]); e.g., a mixing of a dopant material (e.g., tetra-n-butyl ammonium bromide in the case of MBBA) is effective [16]. Sample cells with high f_{cd} (i.e., much larger electric conductivity than that of pure MBBA) should be satisfied with $f_c^* = h f_{cd}^{\alpha}$ ($\alpha = 1.4$, $h = 0.1$), as found in our recent paper [17]. Here, f_c^* stands for a characteristic cutoff frequency of noise giving a crossover between stabilization and destabilization effects on EHCs in superposed fields ($f_{cd} \sim 2450$ Hz in the present cell). In other words, pure noise-induced EHCs can be realized by applying (sufficiently) colored noise with $f_c < f_c^*$.

First, a pure noise-induced typical pattern [WD; see Fig. 4(a)] was observed above a threshold noise voltage V_{N0}. In order to investigate growth of the pattern, we carefully measured the optical intensity $I(x)$ at a selected one-dimensional line (i.e., the x axis) parallel to the wave vector k [18,19]. Figure 1 shows $I(x)$ with an increase of V_N (at a fixed $f_c = 500$ Hz $< f_c^* \sim 5$ kHz). Generally, two (real-image) focus planes for observation of EHCs exit near the upper plate of a cell in the standard optical set [15], which correspond to upward and downward flows for the convection of WDs. We measured $I(x)$ on a fixed (first) focus plane (F_1). Below $V_{N0} \sim 13.04$ V, $I(x)$ does not have observable peaks at expected x_1 and x_2 for F_1. Slightly above V_{N0} ($V_N = 13.06$ V), $I(x)$ becomes periodic with peak $I_{max}(x = x_1, x_2)$ giving an observable pattern (WD). Continuously increasing V_N, I_{max} becomes larger and larger which gives more sharp contrast for the pattern, and other peaks (at $x \sim 52, 105$) also appear owing to the second focus plane (F_2). Here, $I(x)$ reflects the refraction index $n_e(x)$ for extraordinary light passed through the NLC. I_{max} also indirectly indicates a rising angle θ of the director in the NLC cell because of $I = I[n_e(\theta)]$, which means amplitude of the pattern (order parameter).

A normalized optical intensity $I_{max0} = [\{I(x_1)+I(x_2)\}/2 - I_0]/I_0$ was plotted as a function of a normalized control parameter $\varepsilon_N = (V_N^{\,2} - V_{N0}^{\,2})/V_{N0}^{\,2}$, as shown in Fig. 2. Here, I_0 indicates a mean optical intensity along the one-dimensional line. Increasing ε_N, $I_{max0}(\varepsilon_N) \sim 0$ below $\varepsilon_N = 0$ and then continuously increases

into a saturation value ($I_{max0} \sim 0.4$). In this small ε_N region ($\varepsilon_N < 0.07$), I_{max0} can be roughly fitted with $I_{max0}(\varepsilon_N) \sim \sqrt{\varepsilon_N}$, which is theoretically expected [6,13,20]. The saturation of I_{max0} ($\varepsilon_N > 0.07$) could be explained by appearance of secondary instabilities such as oblique rolls or abnormal rolls [20], although they were not dealt with here. Such behavior is almost equivalent to the case of ac-induced WDs, as shown in Fig. 2. Moreover, the behavior of $I(x)$ was independent of the cutoff frequency f_c of noise (see below).

Next, we investigated successive pattern evolutions with increasing V_N (at fixed f_c). A phase diagram was found in the f_c-V_N plane, as shown in Fig. 3. There exists a critical cutoff frequency $f_c^* \sim 5$ kHz dividing frequency regions for appearance of typical patterns and others, similarly to f_{cd} in ac-induced EHCs [5]. In the case of colored noise with $f_c < f_c^*$, surprisingly, a successive pattern transition (WD → FWD → GP → DSM) was observed with increasing *pure noise* intensity V_N. Also, the typical transition from DSM1 to DSM2 [6] was observed in the present noise-induced EHCs, though it is not depicted in Fig. 3. Such transitions have been well known in ac-induced EHCs (for $f < f_{cd}$) [6]. These pure noise-induced patterns [in Fig. 4 (a)-(c)] completely equivalent to ac-induced patterns; no difference was found at least in our experiment.

In the case of (white-like) noise with $f_c > f_c^*$, on the other hand, noise-dominated patterns (NDPs) was found instead of ac-induced chevrons (for $f > f_{cd}$) [5,6]. Well-ordered patterns could not be found; it is quite different from the results of pure noise-induced EHCs in a homeotropically-alligned cell [$\mathbf{n}_0$ = (0,0,1)] [21]. Moreover, the locally turbulent NDPs [Fig. 4(d)] should be differentiated from the wholly turbulent DSMs. The former is originated from white noise with large V_N. In the case of sufficiently white noise ($f_c >> f_c^*$), the threshold for NDPs seems to be constant (~ 65 V).

Finally, the characteristic wavelength λ of noise-induced WDs ($f_c < f_c^*$) was investigated, which was compared to that of ac-induced WDs. The λ is defined as $|x_2 - x_1|$ in Fig. 1. We measured λ as a function of f_c at a fixed $\varepsilon_N = 0.05$ (slightly above V_{N0}). As shown in Fig. 5, λ decreases steeply with increase of f_c. Also, Fig. 6 shows the variation of λ and pattern dynamics. At fixed rather larger ε_N (= 0.11, 0.44) above the threshold V_{N0} ($\varepsilon_N = 0$) for achieving clear contrast of patterns, a spatial-temporal map $I(x,t)$ was measured with switching from f_c = 1k to 200 Hz (t = 100, 450 s) and vise versa (t = 300 s). $I(x,t)$ was expressed as a gray scale image. In the case of relatively small $\varepsilon_N = 0.11$, stationary patterns (WDs) with different λ get settled with time, as shown in Fig. 6(a). Besides, non-stationary (fluctuating) patterns (FWDs) appear at large ε_N = 0.44, as shown Fig. 6(b). They always fluctuate with moving defects, and/or with defect creation-annihilation. Such pattern dynamics are quite similar to the defect turbulence found in ac-induced EHCs [6]. Also, the behavior of $\lambda(f_c)$ is qualitatively equivalent to that of $\lambda(f)$ of ac-induced EHCs [6].

In summary, pure noise can induce a variety of EHCs in NLC systems. The noise should be colored for the instability, satisfying with $f_c < f_c^* = h f_{cd}^{\alpha}$ [17]. In other words, *sufficiently colored* noise ($f_c < f_c^*$) can destabilizes the resting initial state, as an ac field does in CHM. In this point of view, it can be said that CHM corresponds to an instability mechanism for EHCs in *one colored* field (i.e., with one fixed frequency). Regarding the colored noise as a superposition of Fourier modes below f, it may still satisfy the condition of CHM, $2\pi f \tau_\sigma << 1$ and $\tau_d >> \tau_\sigma$, for stable WDs. Here, the director relaxation time $\tau_d = \gamma_1 d^2/(k_{11}\pi^2) \sim 4.15$ s and the charge relaxation time $\tau_\sigma = \varepsilon_0 \varepsilon_\perp / \sigma_\perp \sim 116$ μs were calculated (see ref. [22] for the detail of material constants, γ_1 and k_{11}). Considering the similarity of the structures and thresholds of

the successive patterns in noise- and ac-induced EHCs, it can be said that they are occurred by the power effect [i.e., $<N(t)^2>$ of noise or $<E(t)^2>$ of ac field] rather than f_c of f. On the other hand, white-like noise ($f_c > f_c^*$) cannot induce well-ordered EHCs because of its great randomness. Before reaching to the typical EHCs (chevrons) in the dielectric regime [5,6], the noise induces a locally turbulent pattern [14].

The amplitude of the pattern (WD), the behavior of characteristic wavelength, and the pattern dynamics are governed by the noise intensity V_N. The present results for noise-induced EHCs are almost equivalent to those of ac-induced EHCs, at least in our experiment. Although there are some plausible theoretical models for explaining pure noise induced-pattern formation [23-25], most of them are limited in the threshold determination for a primary instability. The present pattern evolution scenario and dynamics due to strong nonlinearity seem to be beyond the previous theories. Non-trivial noise-induced phenomena reported in various fields [7-9] provide us with useful information for exploiting noise-unavoidable fields such as nanotechnology and neuroscience [26,27].

ACKNOWLEDGMENTS

This study was partly supported by a Grant-in-Aid for Scientific Research from the Ministry of Education, Culture, Sports, Science and Technology of Japan and the Japan Society for the Promotion of Science (No. 18540377).

REFERENCES

1. M.C. Cross and P.C. Hohenberg: Rev. Mod. Phys. **65** (1993) 851.
2. See recent reviews and references therein, for example, T. John, U. Behn, J. Heuer, and R. Stannarius: Phys. Rev. E **71** (2005) 056307; A. Buka, N. Eber, W. Pesch, and L. Kramer: Phys. Rep. **448** (2007) 115.
3. R. Williams: J. Chem. Phys. **39** (1963) 384.
4. E. F. Carr: Mol. Cryst. Liq. Cryst. **7** (1969) 256, W. Helfrich: J. Chem. Phys. **51** (1969) 4092.
5. L. M. Blinov: *Electro-Opical and Magneto-Optical Properties ofLiquid Crystals* (Wiley, Chichester, U.K., 1983).
6. S. Kai and W. Zimmermann: Prog. Theor. Phys. Supp. **99** (1989) 458.
7. W. Horsthemke and R. Lefever: *Noise-Induced Transitions* (Springer-Verlag, Berlin, 1984).
8. J. Garcia-Ojalvo and J. M. Sancho: *Noise in Spatially Extended Systems* (Springer-Verlag, New York, 1999).
9. F. Sagues, J. M. Sancho, and J. Garcia-Ojalvo: Rev. Mod. Phys. **79** (2007) 829.
10. S. Kai, T. Kai, M. Takata, and K. Hirakawa: J. Phys. Soc. Jpn. **47** (1979) 1379; H. Brand and A. Schenzle: J. Phys. Soc. Jpn. **48** (1980) 1382; S. Kai, H. Fukunaga, and H. Brand: J. Phys. Soc. Jpn. Lett. **56** (1987) 3759; J. Stat. Phys. **54** (1989) 1133; S. Kai, M. Imasaki, S. Yamaguchi, and F. Sagues: *Research of Pattern Formation*, edited by R. Takaki (KTK Scientific Publishers, Tokyo, 1994), p.343.
11. T. Kawakubo, A. Yanagita, and S. Kabashima: J. Phys. Soc. Jpn. **50** (1981) 1451.

12. R. Graham and A. Schenzle: Phys. Rev. A **26** (1982) 1676.
13. U. Behn and R. Müller: Phys. Lett. **113A** (1985) 85; R. Müller and U. Behn, Z. Physik B **69** (1987) 185; U. Behn, A. Lange, and T. John: Phys. Rev. E **58** (1998) 2047; T. John, R. Stannarius, and U. Behn: Phys. Rev. Lett. **83** (1999) 749; T. John, U. Behn, and R. Stannarius: Phys. Rev. E **65** (2002) 046229.
14. J. -H. Huh: J. Phys. Soc. Jpn. **76** (2007) 033001; J. -H. Huh and S. Kai, J. Phys. Soc. Jpn. **77** (2008) 083601; J. Phys. Soc. Jpn. **78** (2009) 083601; J. -H. Huh, A. Kuribayashi, and S. Kai: Phys. Rev. E **80** (2009) 066304.
15. K. Kondo, M. Arakawa, A. Fukuda, and E. Kuze: Jpn. J. Appl. Phys. **22** (1983) 394.
16. J. -H. Huh, Y. Hidaka, Y. Yusuf, and S. Kai: Phys. Rev. E **66** (2002) 031705.
17. J. -H. Huh and S. Kai (private communication).
18. S. P. Trainoff and D. S. Cannell: Phys. Fluids, **14** (2002) 1340.
19. T. John, U. Behn, and R. Stannarius: Eur. Phys. J. B **35** (2003) 267.
20. E. Plaut and W. Pesch: Phys. Rev. E **59** (1999) 1747.
21. J. -H. Huh and S. Kai: J. Phys. Soc. Jpn. **78** (2009) 043601.
22. E. Bodenschatz, W. Zimmermann, and L. Kramer: Prog. J. Phys. (Paris), **49** (1988) 1875.
23. C. Van den Broeck, J. M. R. Parrondo, and R. Toral: Phys. Rev. Lett. **73** (1994) 3395.
24. J. M. R. Parrondo, C. Van den Broeck, J. Buceta, and J. de la Rubia: Physica A, **224** (1996) 153.
25. J. Buceta, M. Ibanes, J. M. Sancho, and K. Lindenberg: Phys. Rev. E **67** (2003) 021113.
26. G. Stegemann, A. G. Balanov, and E. Schöll: Phys. Rev. E **71** (2005) 016221.
27. G. M. Süel, J. Garcia-Ojalvo, L. M. Liberman, and M. B. Elowitz: Nature **440** (2006) 545; N. Rosenfeld, J. W. Young, U. Alon, P. S. Swain, and M. B. Elowitz: Science **307** (2005) 1962.

Figure Captions

(Color) FIG. 1 One-dimensional optical intensity $I(x)$ with increase of noise intensity V_N. $I(x)$ represents the amplitude of a pattern (WD; see Fig. 2) in an arbitrarily selected line parallel to the wave vector of WDs. The increasing peaks $I(x_1, x_2)$ indicate the upward flows of vortices for a WD at the first real focus plane [15].

FIG. 2 Normalized peak intensity I_{max0} as a function of a control parameter [$\varepsilon_N = (V_N{}^2 - V_{N0}{}^2)/V_{N0}{}^2$ for noise-induced EHCs (f_c = 500 Hz) and $\varepsilon = (V^2 - V_c^2)/V_c^2$ for ac-induced EHCs (f = 30 Hz of a sinusoidal field)]. Here, V_{N0} and V_c indicate the threshold voltages for both EHCs, respectively.

FIG. 3 A phase diagram in f_c-V_N plane. The typical patterns (found in ac-induced EHCs) are also realized in the present noise-induced EHCs (f_c < a characteristic cutoff frequency f_c^* ~ 5 kHz). See their real patterns in Fig.4.

FIG. 4 Typical patterns in pure noise-induced EHCs. (a) Williams domain (WD), (b) fluctuating Williams domain (FWD), (c) grid pattern (GP), (d) noise-dominated pattern (NDP).

FIG. 5 Cutoff frequency f_c-dependence of the characteristic wavelength λ for WDs (at fixed ε_N).

FIG. 6 Spatial-temporal map $I(x,t)$ with switching f_c (between f_c = 1k and 200 Hz) at a fixed ε_N = 0.11 for WD (a) and 0.44 for FWD (b). For example, switching f_c from 1k to 200 Hz was done at t = 100 s and vice versa at t = 300 s. See also Fig. 5.

Fig.1

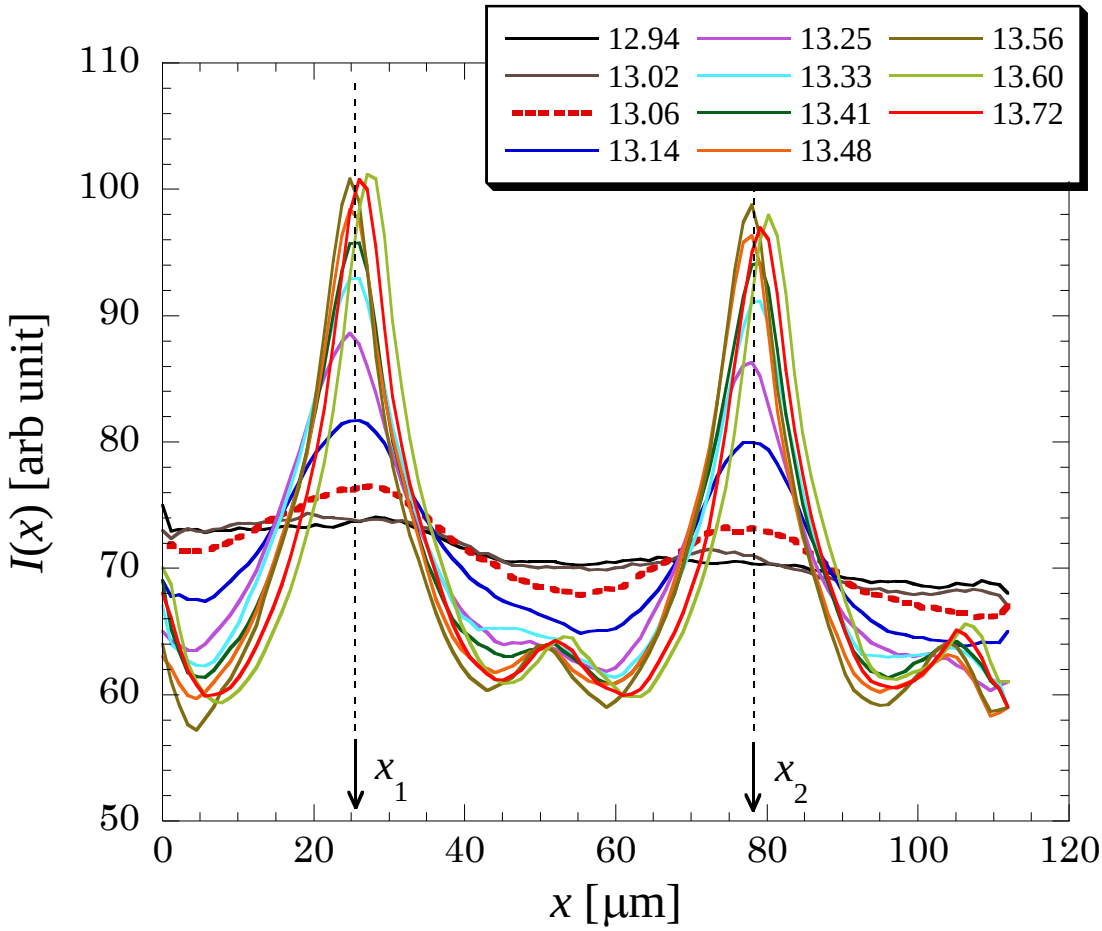
12.94
13.02
13.06
13.14
13.25
13.33
13.41
13.48
13.56
13.60
13.72
110
100
90
80
70
60
50
0
20
40
60
80
100
120
I(x) [arb unit]
x [μm]
x1
x2

Fig.2

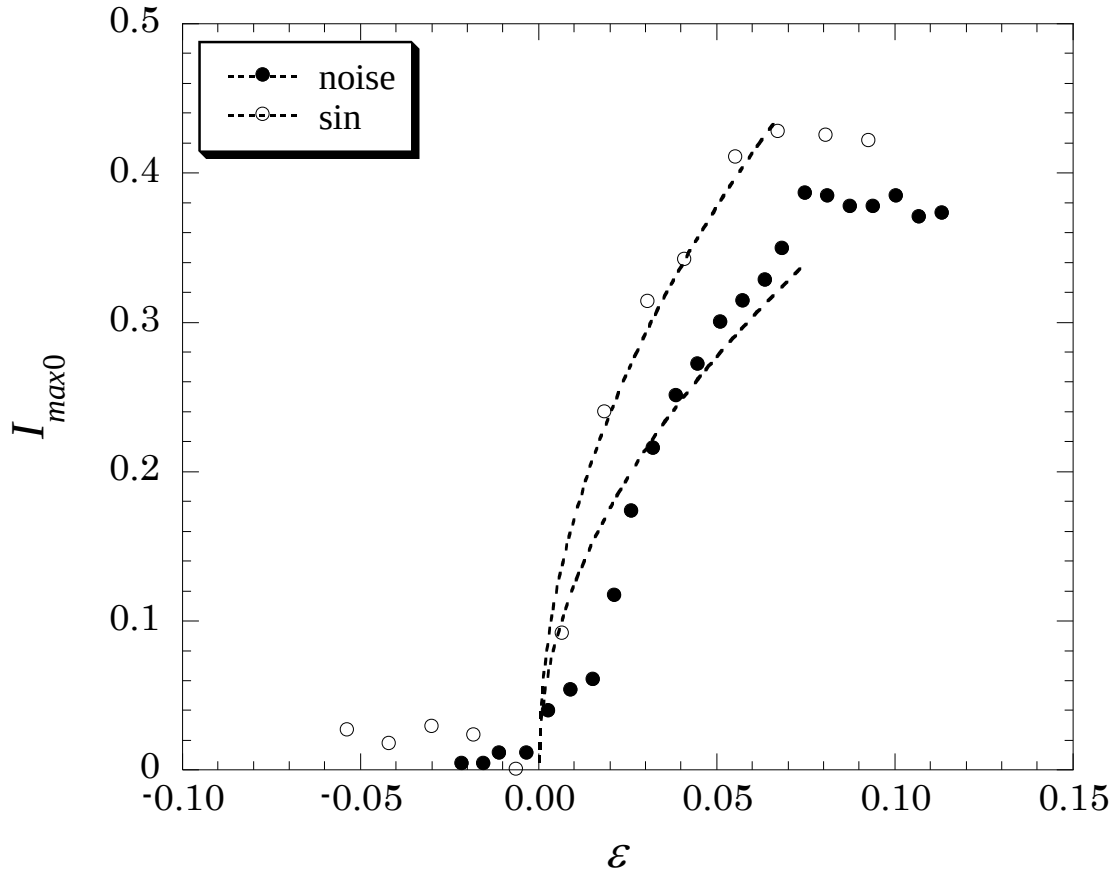
noise
sin
0.5
0.4
0.3
0.2
0.1
0
-0.10
-0.05
0.00
0.05
0.10
0.15
I_{max0}
ε

Fig.3

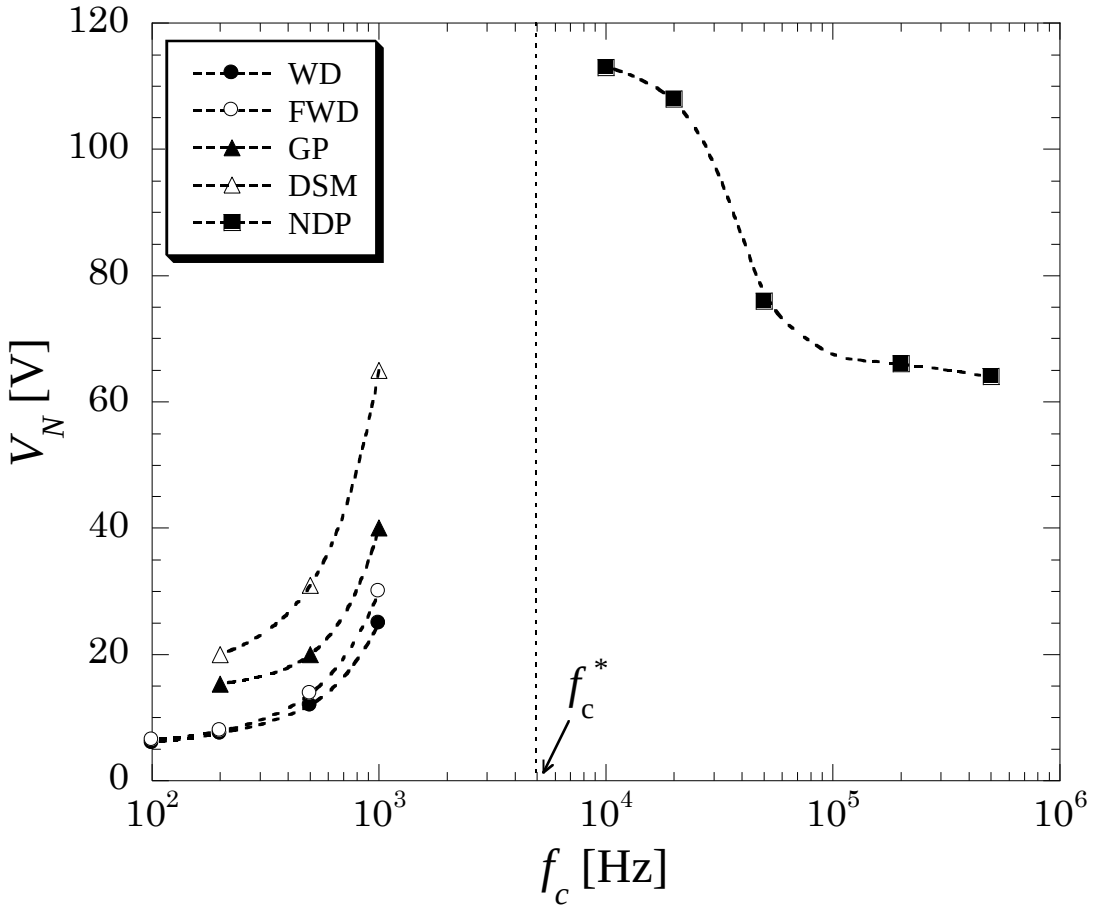
120
100
80
60
40
20
0
V_N [V]
WD
FWD
GP
DSM
NDP
f_c^*
10^2
10^3
10^4
10^5
10^6
f_c [Hz]

Fig.4

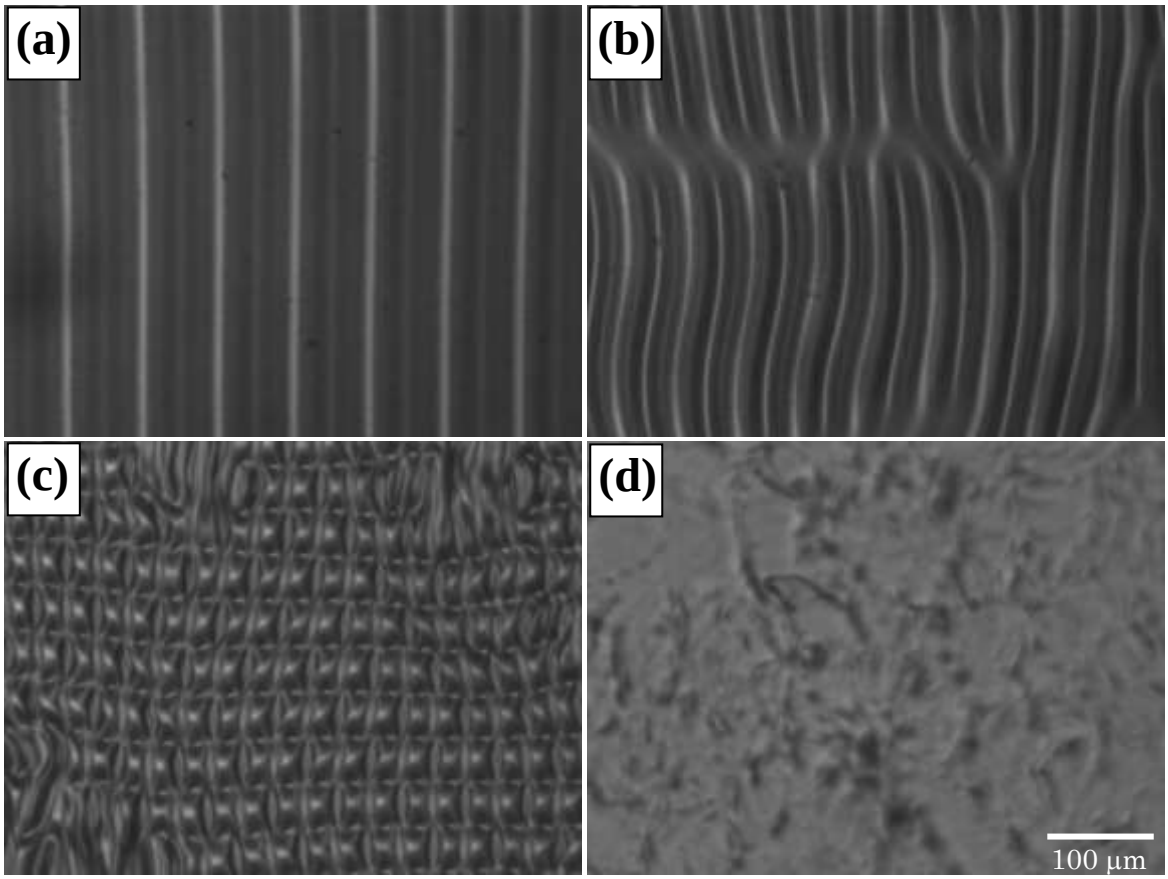

Fig.5

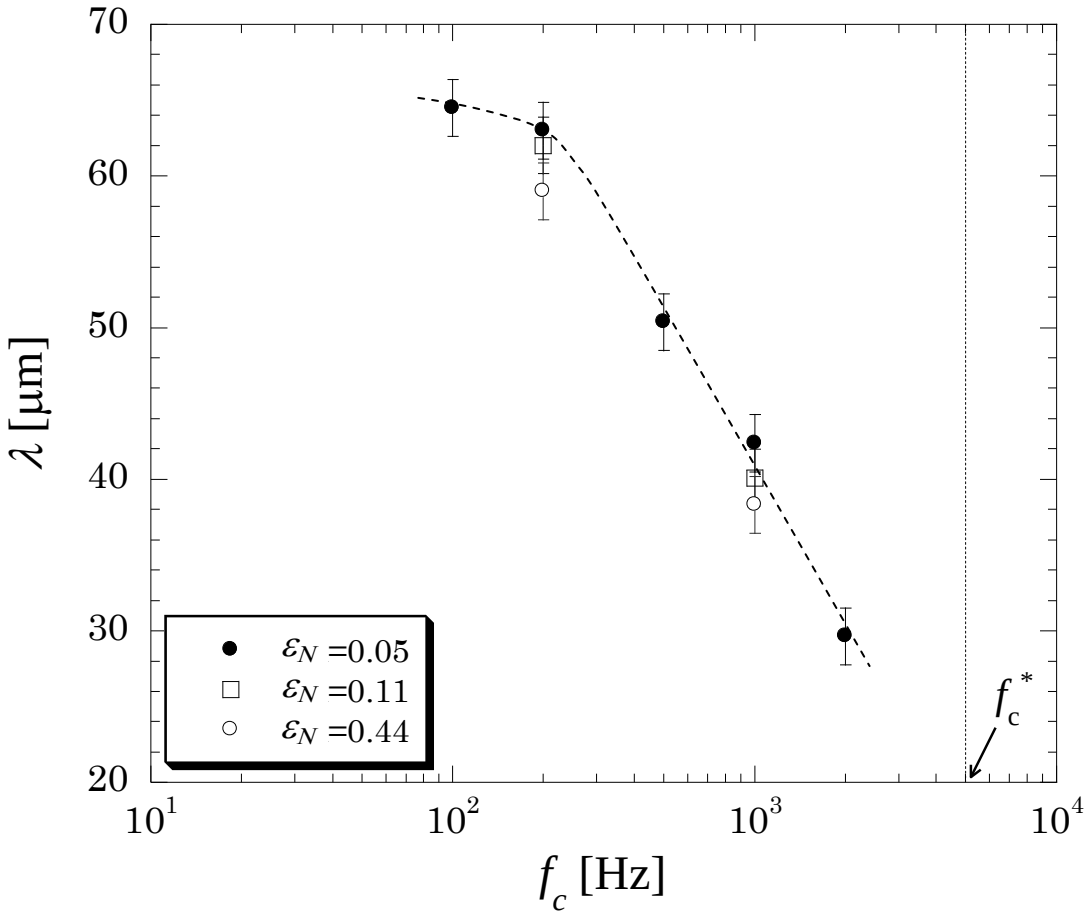

Fig.6

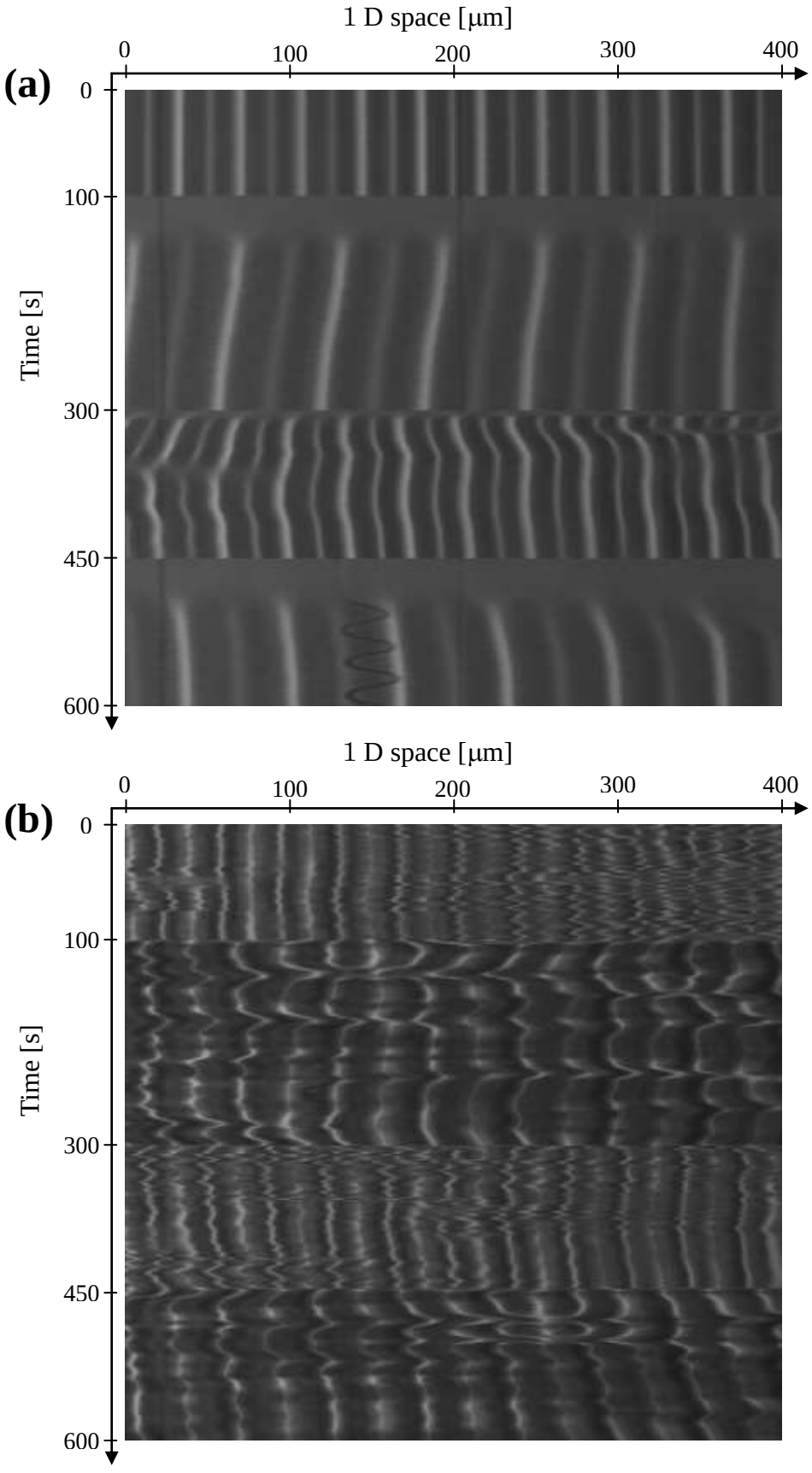
(a)
1 D space [μm]
0
100
200
300
400
Time [s]
0
100
300
450
600
(b)
1 D space [μm]
0
100
200
300
400
Time [s]
0
100
300
450
600